

# Green Synthesis of Iron Oxide Nanoparticles ( $\text{Fe}_3\text{O}_4$ -NPs) using *Azadirachta Indica* Aqueous Leaf Extract

Nurul Izza Taib<sup>1\*</sup>, Famiza Abdul Latif<sup>2</sup>, Zakiah Mohamed<sup>2</sup>, Nur Diyana Syazwani Zambr<sup>2</sup>

<sup>1</sup>Faculty of Applied Sciences, Universiti Teknologi MARA, Perak Branch, Tapah Campus, 35400 Tapah Road, Perak, Malaysia

<sup>2</sup>Faculty of Applied Sciences, Universiti Teknologi MARA (UiTM), 40450, Shah Alam, Selangor, Malaysia

\*Corresponding author E-mail: [izza257@uitm.edu.my](mailto:izza257@uitm.edu.my)

## Abstract

On treatment of aqueous solutions of ferrous and ferric salts in alkaline medium with *Azadirachta indica* leaf extract, the rapid formation of stable iron oxide nanoparticles ( $\text{Fe}_3\text{O}_4$ -NPs) or also known as magnetite nanoparticles is observed to occur. In contrast to previously reported co-precipitation approaches, our synthesis method had utilized a much cheaper and less toxic iron precursor with environmentally benign and non-toxic *Azadirachta indica* leaf extract was used as a reducing and stabilizing agent. It was found that the presence of various biomolecules such as flavonoids and terpenoids of the aqueous leaf extract plays a major role for the formation of  $\text{Fe}_3\text{O}_4$ -NPs through infrared spectra analysis. The formation was further confirmed with strong characteristic peak observed at 249 nm for  $\text{Fe}_3\text{O}_4$ -NPs through UV-Vis spectroscopy. Besides, the shape was mostly spherical and oval. X-Ray Diffraction (XRD) analysis revealed the purity of synthesized  $\text{Fe}_3\text{O}_4$ -NPs with crystalline cubic structure phase. Transmission Electron Microscopy (TEM) results illustrated that the size and diameter was in the range from 9-14 nm which agrees with calculated Scherrer equation with average diameter of around 11 nm. Vibrating Sample Magnetometer (VSM) analysis indicated that the samples exhibit superparamagnetic with magnetization value was 82 emu/g. Results confirmed this protocol as a simple, rapid, one-step, eco-friendly, non-toxic and hence can be potentially used in various biomedical applications such as magnetic targeting drug delivery system.

**Keywords:** *Azadirachta indica*; eco-friendly; iron oxide nanoparticles; magnetite; non-toxic.

## 1. Introduction

Due to environmental concerns, the green route methods have become increasingly popular to synthesize nanoparticles as they are well known to be environmentally-friendly and help to reduce harmful effects on environment [1]. Nanoparticle is a particle in the nanometre scale which usually in the range of 1 to 100 nm [2], [3]. During the last decade, the exploration of iron oxide nanoparticles ( $\text{Fe}_3\text{O}_4$ -NPs) has earned numerous attentions as a consequence of their unique characteristics and various potential applications in biomedicine field [4]–[6]. Besides, iron oxide nanoparticles also are frequently encountered in most applications because of their biocompatibility, superparamagnetism, high saturation magnetization and low toxicity [7]. They are also the only type of magnetic nanoparticles that are approved by Food and Drug Administration (FDA) for clinical use [7], [8]. The various biomedical applications include magnetic resonance imaging (MRI) contrast agents, hyperthermia, magnetic targeted drug delivery, tissue specific release of therapeutic agents and magnetic field assisted radionuclide therapy [7], [9]. The synthesized nanoparticles will be further studied for application in magnetic targeting drug delivery system.

Hence, numerous methods were investigated for synthesis of  $\text{Fe}_3\text{O}_4$ -NPs with the aim to produce nanoparticles of different sizes, shapes, controlled dispersity and safer to be used in biomedical applications like for magnetic targeting drug delivery system. Among them are sol gel process, co-precipitation, hydrothermal techniques, thermal decomposition, and microemulsion route [10].

However, the drawbacks of these methods include low production rates, high energy consumption and high cost, as well as the release of a large amount of toxic byproducts, the usage of precursors and surfactants in organic solvent that are toxic enough to pollute the environment [11]–[13].

Thus, there is a growing need to develop environmentally benign nanoparticle synthesis that does not require harmful chemicals in the synthesis protocol. Synthesis of nanoparticles by plant extracts is an exciting possibility that is under exploration and exploitation. Green synthesis is not only able to reduce environmental impact but attractive enough if they are intended for invasive applications in medicine. It can be efficient alternative to produce large quantities of nanoparticles that are eco-friendly, non-toxic, simpler and less expensive. The ready availability of reducing and capping agent from the resource plant itself is an additional advantage of this system. In this study, we report the synthesis of  $\text{Fe}_3\text{O}_4$ -NPs by one-pot reaction by the reduction of aqueous  $\text{Fe}^{3+}$  and  $\text{Fe}^{2+}$  ions with the *Azadirachta Indica* leaf extract in an alkaline medium. *Azadirachta Indica* or also known as neem has medicinal properties such as antibacterial, antifungal and anthelmintic [14]. The alkaline medium in weak base also is more effective compared to using strong base. The water soluble  $\text{Fe}_3\text{O}_4$ -NPs were characterized by Fourier Transform Infrared (FTIR), Ultraviolet-Visible Spectroscopy (UV-Vis), X-Ray Diffraction (XRD), Transmission Electron Microscopy (TEM) and Vibrating Scanning Magnetometer (VSM).

## 2. Materials and Methods

### 2.1. Materials

In this work, the fresh leaves of *Azadirachta indica* (neem leaves) were collected from Batu Caves, Selangor, Malaysia. Iron (II) chloride tetrahydrate ( $\text{FeCl}_2 \cdot 4\text{H}_2\text{O}$ ), iron (III) chloride hexahydrate ( $\text{FeCl}_3 \cdot 6\text{H}_2\text{O}$ ) and 25% ammonium hydroxide ( $\text{NH}_4\text{OH}$ ) were purchased from Sigma Aldrich Chemical Company. All chemicals were of analytical grade and utilized without further purification.

### 2.2. Methods

#### 2.2.1 Preparation of Azadirachta Indica Aqueous Leaf Extract

The leaves were thoroughly washed several times with distilled water to remove dust and then air dried at room temperature to remove the remaining moisture. Then, the dried leaves were cut into small pieces and made into powder. Approximately, 5 g of neem leaf powder was added into 100 mL sterile distilled water and the mixture was heated at constant temperature of 80 °C. Then, the mixture was left to cool at room temperature before vacuum-filtered through Whatman filter paper No. 1 to obtain extract. The extract was stored at 4 °C until further use.

#### 2.2.2 Synthesis of Iron Oxide Nanoparticles ( $\text{Fe}_3\text{O}_4$ -NPs) via Co-Precipitation Method

In a typical procedure, 0.40 g iron (II) chloride tetrahydrate ( $\text{FeCl}_2 \cdot 4\text{H}_2\text{O}$ ) and 1.10 g of iron (III) chloride hexahydrate ( $\text{FeCl}_3 \cdot 6\text{H}_2\text{O}$ ) with 1:2 molar ratio were dissolved in 100 mL of sterile deionized water under nitrogen atmosphere. Following this, the resulting mixture was heated up to 80 °C under mild stirring for 10 minutes. Then, 5 mL of aqueous neem leaf extract was added slowly into the resulting mixture and subsequently 20 mL of 25% ammonium hydroxide ( $\text{NH}_4\text{OH}$ ) was added into the reaction mixture drop by drop using burette under vigorous stirring for 30 minutes. The instantaneous black color appearance indicated the formation of  $\text{Fe}_3\text{O}_4$ -NPs. After 30 minutes, the solution was poured into a beaker and magnetic decantation was carried out in order to remove the supernatant. The intense black precipitate  $\text{Fe}_3\text{O}_4$ -NPs was then washed with 15 mL deionized water and centrifuged at 5000 rpm for 10 minutes. The supernatant was removed. The product was washed again with 10 mL of deionized water followed by centrifugation. The supernatant was removed again. The pellet was transferred to a vial and 10 mL deionized water was added. The obtained black powder was freeze dried overnight and subjected for further characterization.

#### 2.2.3 Characterization

UV-Vis spectral analysis was done by using Perkin Elmer UV-Vis spectrometer Lambda 35 with a resolution of 1 nm between 200 and 600 nm. The size and the morphology of the  $\text{Fe}_3\text{O}_4$ -NPs was observed by means of a transmission electron microscopy (TEM) using Technai G2 20S Twin TEM, Netherland working at 200 kV. The samples were prepared by drop deposition of a diluted solution onto a carbon-coated copper grid. X-ray powder diffraction (XRD) was used to analyze the structure and identify the phase purity of  $\text{Fe}_3\text{O}_4$  compounds. The samples were placed on a flat plate while intensity data were collected as a function of the Bragg angle,  $\theta$ , in the range  $2\theta = 10^\circ$  to  $70^\circ$  with a step size of  $0.013^\circ$  using a PAN analytical X'pert PRO diffractometer in Bragg-Brentano geometry using  $\text{Cu K}_\alpha$  radiation wavelength  $\lambda_{\alpha 1} = 1.5405 \text{ \AA}$ ,  $\lambda_{\alpha 2} = 1.5443 \text{ \AA}$ . The structures were refined with the full-profile Rietveld method using GSAS [15] with the EXPGUI interface [16]. Fourier transform infrared (FTIR) spectra were collected using a Perkin Elmer FTIR spectrophotometer using KBr pellet

method with a range of  $4000\text{--}400 \text{ cm}^{-1}$ . The magnetic properties of the prepared  $\text{Fe}_3\text{O}_4$  were revealed using a vibrating sample magnetometer (VSM, Lake Shore 7404) at room temperature 300 K. The magnetization measurements,  $M$  as a function of applied field ( $H$ ) were measured under external magnetic fields up to  $\pm 14000 \text{ Oe}$ .

## 3. Results and Discussion

### 3.1. The Study of Fourier Transform Infrared Spectrum (FTIR) of Azadirachta Indica Leaf Extract and Synthesized $\text{Fe}_3\text{O}_4$ -NPs

FTIR analysis of pure *Azadirachta indica* leaf extract (Fig. 1) and the synthesized  $\text{Fe}_3\text{O}_4$ -NPs (Fig. 2) were carried out to identify the potential functional groups of the biomolecules which are flavanones and terpenoids in the *Azadirachta indica* leaf extract which are responsible for the stabilization of iron oxide nanoparticles. The strong absorption band around  $3324 \text{ cm}^{-1}$  is due to the N-H stretching and bending vibration of amine group  $\text{NH}_2$  and the overlapping of the stretching vibration of OH attributed to water and *Azadirachta indica* leaf extract molecules. The decrease in intensity at  $3416 \text{ cm}^{-1}$  implies the involvement of functional groups of *Azadirachta indica* in the reduction process. The absorption peak at  $1633 \text{ cm}^{-1}$  (Fig. 1) can be assigned to amide C=O stretching indicating the presence of  $-\text{COOH}$  group in the *Azadirachta indica* leaf extract. The decreasing intensity at  $1633 \text{ cm}^{-1}$  (Fig. 2) signifies the involvement of amide C=O stretching in the reduction process. Meanwhile, the absorption peak at  $2429 \text{ cm}^{-1}$  (Fig. 2) corresponds to alkyne group presents in phytoconstituents of extracts. Hence, the presence of these functional groups validates that flavanones or terpenoids molecules were chemically bonded to the surface of  $\text{Fe}_3\text{O}_4$ -NPs. It is evident from the small shifts in the peak position (Fig. 2) that the flavanones or terpenoids adsorbed on the surface of iron oxide nanoparticles and capping effect did enhance  $\text{Fe}_3\text{O}_4$ -NPs intermolecular interaction.

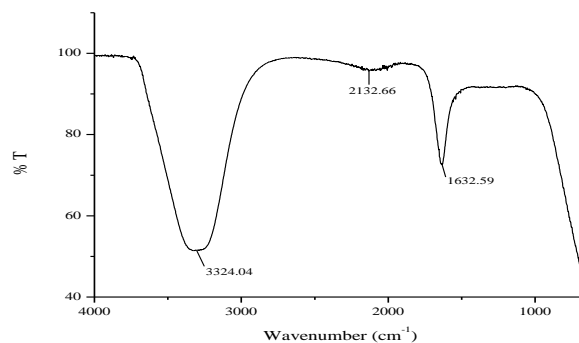


Fig. 1: FTIR spectrum of aqueous leaf extract of *Azadirachta indica*

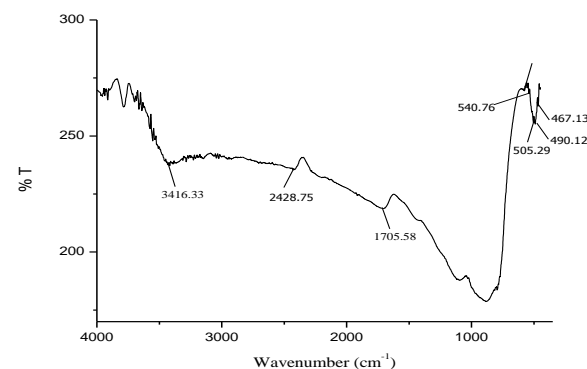


Fig. 2: FTIR spectrum of the synthesized  $\text{Fe}_3\text{O}_4$ -NPs

It was also observed the occurrence of strong peaks at  $541\text{ cm}^{-1}$ ,  $505\text{ cm}^{-1}$ ,  $490\text{ cm}^{-1}$  and  $467\text{ cm}^{-1}$  denote to the Fe-O stretching band of iron oxide nanoparticles. These results are comparable with previous literature that also used neem leaf extract but with a different alkaline medium in which the iron oxide nanoparticles peaks were observed at  $513\text{ cm}^{-1}$ ,  $460\text{ cm}^{-1}$  and  $440\text{ cm}^{-1}$  [17]. Therefore, these results confirmed that the presence of various biomolecules such as flavonoids and terpenoids in the neem leaf extracts played an important role in the reduction and stability of  $\text{Fe}_3\text{O}_4$ -NPs [1].

### 3.2. The Study of Ultraviolet Visible Spectroscopy (UV-Vis)

The synthesis of  $\text{Fe}_3\text{O}_4$ -NPs was confirmed by the UV-visible spectral analysis (Fig. 3). A strong peak at 249 nm region was observed due to the excitation of surface plasmon vibrations in the iron oxide nanoparticles. It is the characteristic absorption peak for iron oxide nanoparticles as reported by literature that obtained strong peak in between 230-250 nm [17], [18]. Hence, it was proven that  $\text{Fe}_3\text{O}_4$ -NPs also can be synthesized using this one step reaction only.

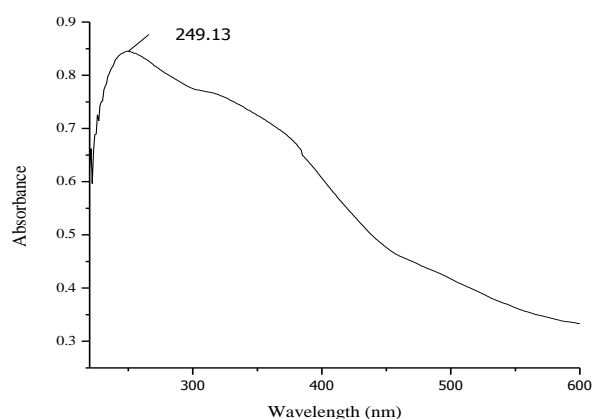


Fig. 3: UV-Visible absorption spectra of  $\text{Fe}_3\text{O}_4$ -NPs

### 3.3. The Study of X-Ray Diffraction (XRD)

Fig. 4 shows the X-Ray powder diffractions of  $\text{Fe}_3\text{O}_4$  at room temperature. The XRD data clearly confirm the crystalline phase of  $\text{Fe}_3\text{O}_4$ . From the X-ray diffraction patterns, six series of characteristic peaks at  $2\theta = 30^\circ$ ,  $36^\circ$ ,  $43^\circ$ ,  $54^\circ$ ,  $57^\circ$  and  $63^\circ$  which correspond to (220), (311), (400), (422), (511) and (440) were observed. All the diffraction peaks were indexed as a cubic structure of  $\text{Fe}_3\text{O}_4$  phase and the calculated lattice parameter of the sample was  $8.38\text{ \AA}$  is in good agreement with the standard data (JCPDS file PDF:19-0627). The observed lattice parameter is similar with the reported in the literature [19]. No other characteristic peaks are detected in this pattern, indicating that the purity of the synthesized sample.

Based on the XRD data, the particle size of iron oxide nanoparticles can be calculated using Scherrer's formula as shown in Equation 1.

$$D = \frac{0.9 \times \lambda}{\Delta \cos \theta} \quad (1)$$

where  $D$  is the crystallite size,  $0.9$  is a constant shape factor,  $\lambda$  is the X-ray wavelength,  $\Delta$  is the full width at half maximum (FWHM) and  $\theta$  is the Bragg's angle. The calculated average particle size of  $\text{Fe}_3\text{O}_4$  was found to be  $11\text{ nm}$ .

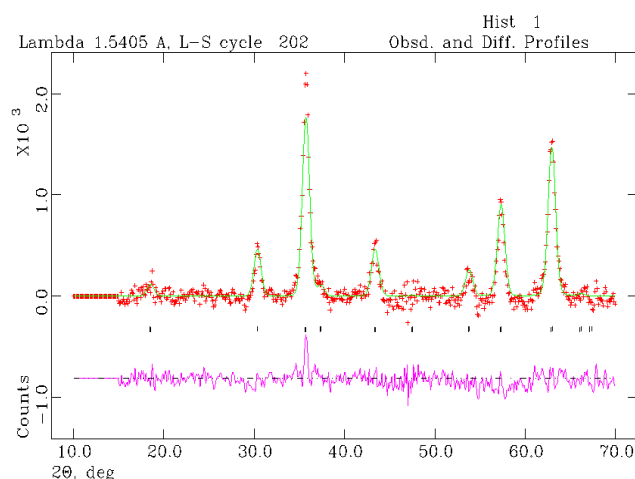


Fig. 4: Rietveld refinements of  $\text{Fe}_3\text{O}_4$  against XRD data. Observed, calculated and the difference profiles are represented by red crosses, green lines and pink lines, respectively

### 3.4. The Study of Transmission Electron Microscope (TEM)

Shown in Fig. 5 is a representative TEM micrograph of  $\text{Fe}_3\text{O}_4$ -NPs. As shown in Fig. 5, the particle size distribution of the  $\text{Fe}_3\text{O}_4$ -NPs is found to be in the range of  $9\text{--}14\text{ nm}$ . It reveals that the  $\text{Fe}_3\text{O}_4$ -NPs are well dispersed and predominantly spherical in shape, while some of the NPs were found to be having structures of irregular shape. The particle size agrees with that calculated from Scherrer equation with average diameter of around  $11\text{ nm}$ . This result is comparable with previous literature [17] that used the same green route method but differed in the use of alkaline medium in which they used sodium hydroxide. The good correlation between particle sizes obtained from Scherrer equation and TEM supports the crystalline structure of the iron nanoparticles.

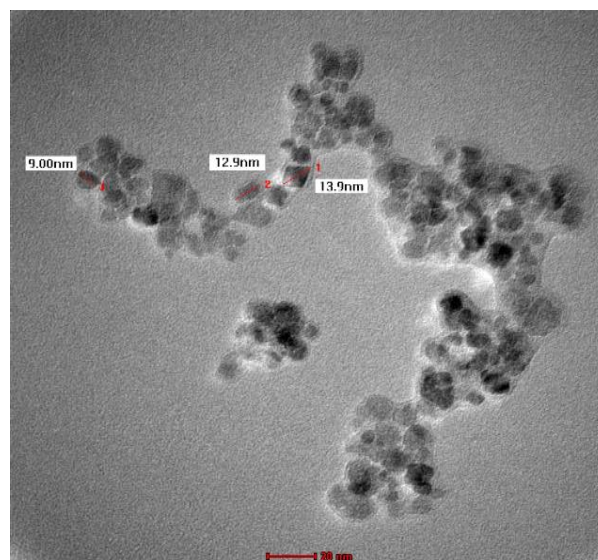


Fig. 5: TEM images of  $\text{Fe}_3\text{O}_4$ -NPs from *Azadirachta indica* leaf extract

### 3.5. The Study of Vibrating Sample Magnetometer (VSM)

Fig. 6 shows the variation of magnetization ( $M$ ) versus the applied magnetic field ( $H$ ) measured by Vibrating Sample Magnetometer (VSM) at  $300\text{ K}$ . No hysteresis loops were observed. The magnetization increases with increasing magnetic field and saturates at higher magnetic fields. The plot indicates that the samples exhibit superparamagnetic behavior with approximately zero remanence

and coercivity. The saturation magnetization ( $M_s$ ), determined by using the law approaches to saturation. The magnetization of  $\text{Fe}_3\text{O}_4$  was 82 emu/g which is less than that of the actual magnetization of the  $\text{Fe}_3\text{O}_4$  is 92 emu/g [20]. The decrease of the saturation is ascribed to the size effect in which the smaller the size of the nanoparticles, the lower the saturation magnetization value. The saturation magnetization ( $M_s$ ) of the  $\text{Fe}_3\text{O}_4$  indicates the presence of non-magnetic surface layers resulting from the strong chemical attachment of the stabilizing agent of *Azadirachta indica* leaf extract to the  $\text{Fe}_3\text{O}_4$ 's surface, also observed by FTIR spectroscopy.

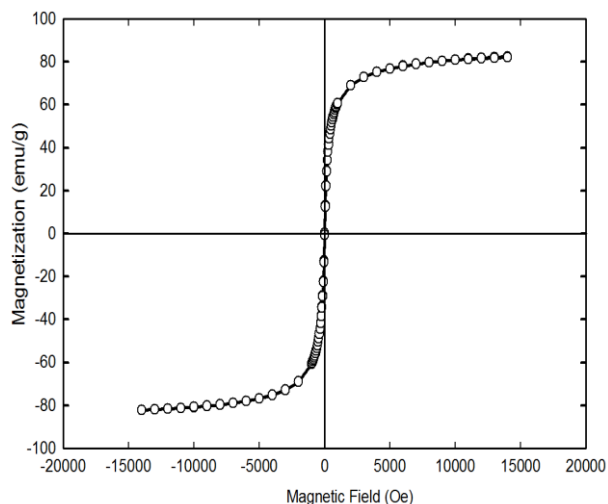


Fig. 6: Magnetization versus applied magnetic field for  $\text{Fe}_3\text{O}_4$ -NPs

### 3.6. Macroscopic Observation

The  $\text{Fe}_3\text{O}_4$ -NPs exhibited a magnetic property in the presence of a magnetic field. It was observed that  $\text{Fe}_3\text{O}_4$ -NPs were attracted towards external magnetic field when magnetic block was placed next to it as demonstrated in Fig. 7. The powder also was seen to move along when the magnetic block was moved around the vial. This was not observed without external magnetic field.



Fig. 7: Magnetic behavior of iron oxide nanoparticles

## 4. Conclusion

In this work, we had successfully demonstrated that crystalline  $\text{Fe}_3\text{O}_4$ -NPs can be synthesized in a one-step reaction using a green facile approach with the less use of hazardous and toxic chemicals in which contributes to more environmentally and eco-friendly approach. The use of *Azadirachta indica* leaf extract as reducing and stabilizing agent also has been proven to be effective and efficient according to FTIR analysis. The results of the  $\text{Fe}_3\text{O}_4$  have been characterized to be crystalline in nature by XRD, and all the diffraction peaks can be indexed to the pure cubic phase. The TEM result confirmed the size of nanoparticles are in the range of

9-14 nm. The magnetic properties are measured by the vibration sample magnetometer (VSM) and the particles have the properties of the saturation magnetization ( $M_s$ ) of 82 emu/g. The magnetization measurements confirm that the samples are superparamagnetic. In summary,  $\text{Fe}_3\text{O}_4$ -NPs synthesized in this work could be useful for biomedical applications as magnetic targeting drug delivery system or contrasting agents due to their small particle size and superparamagnetic property.

## Acknowledgement

The authors would like to acknowledge the financial support from Universiti Teknologi Mara (UiTM), Malaysia (600-IRMI/MYRA 5/3/LESTARI (048/2017)) and Ministry of Science, Technology and Innovation Malaysia (MOSTI) for financial support through funding 600-IRMI/FRGS 5/3 (046/2017). The microscopy analysis was carried out using facilities at the Microscopy and Microanalysis facility at Faculty of Pharmacy, Universiti Teknologi MARA (UiTM), Puncak Alam Campus. Meanwhile, VSM was performed at Universiti Kebangsaan Malaysia.

## References

- [1] S. Ahmed, Saifullah, M. Ahmad, B. L. Swami, and S. Ikram, "Green Synthesis of Silver Nanoparticles using *Azadirachta Indica* Aqueous Leaf Extract," *J. Radiat. Res. Appl. Sci.*, vol. 9, no. 1, pp. 1-7, 2016.
- [2] H. A. Salam, P. Rajiv, M. Kamaraj, P. Jagadeeswaran, S. Gunalan, and R. Sivaraj, "Plants : Green Route for Nanoparticle Synthesis," *Int. Res. J. Biol. Sci.*, vol. 1, no. 5, pp. 85-90, 2012.
- [3] L. Tong, M. Zhao, S. Zhu, and J. Chen, "Synthesis and Application of Superparamagnetic Iron Oxide Nanoparticles in Targeted Therapy and Imaging of Cancer," *Front. Med.*, vol. 5, no. 4, pp. 379-387, 2011.
- [4] S. Laurent, D. Forge, M. Port, a Roch, C. Robic, L. V Elst, and R. N. Muller, "Magnetic Iron Oxide Nanoparticles: Synthesis, Stabilization, Vectorization, Physicochemical Characterizations, and Biological Applications (vol 108, pg 2064, 2008)," *Chem. Rev.*, vol. 108, no. 6, pp. 2064-2110, 2008.
- [5] Q. A. Pankhurst, J. Connolly, J. S. K, and J. Dobson, "Applications of Magnetic Nanoparticles in Biomedicine," *J. Phys. D. Appl. Phys.*, vol. 36, pp. R167-R181, 2003.
- [6] C. Xu and S. Sun, "New Forms of Superparamagnetic Nanoparticles for Biomedical Applications," *Adv. Drug Deliv. Rev.*, vol. 65, no. 5, pp. 732-743, 2013.
- [7] S. F. Chin, S. C. Pang, and C. H. Tan, "Green Synthesis of Magnetite Nanoparticles (via Thermal Decomposition Method) with Controllable Size and Shape," *J. Mater. Environ. Sci.*, vol. 2, no. 3, pp. 299-302, 2011.
- [8] S. Purushotham and R. V. Ramanujan, "Thermoresponsive Magnetic Composite Nanomaterials for Multimodal Cancer Therapy," *Acta Biomater.*, vol. 6, no. 2, pp. 502-510, 2010.
- [9] M. Mahmoudi, S. Sant, B. Wang, S. Laurent, and T. Sen, "Superparamagnetic Iron Oxide Nanoparticles (Spions): Development, Surface Modification And Applications in Chemotherapy," *Adv. Drug Deliv. Rev.*, vol. 63, no. 1-2, pp. 24-46, 2011.
- [10] A. H. Lu, E. L. Salabas, and F. Schüth, "Magnetic Nanoparticles: Synthesis, Protection, Functionalization, and Application," *Angew. Chemie - Int. Ed.*, vol. 46, no. 8, pp. 1222-1244, 2007.
- [11] A. K. Mittal, Y. Chisti, and U. C. Banerjee, "Synthesis of Metallic Nanoparticles using Plant Extracts," *Biotechnol. Adv.*, vol. 31, no. 2, pp. 346-356, 2013.
- [12] S. Saif, A. Tahir, and Y. Chen, "Green Synthesis of Iron Nanoparticles and Their Environmental Applications and Implications," *Nanomaterials*, vol. 6, no. 11, p. 209, 2016.
- [13] P. Mohanpuria, N. K. Rana, and S. K. Yadav, "Biosynthesis of Nanoparticles: Technological Concepts and Future Applications," *J. Nanoparticle Res.*, vol. 10, no. 3, pp. 507-517, 2008.
- [14] M. Pattanayak and P. L. Nayak, "Ecofriendly Green Synthesis Of Iron Nanoparticles From Various Plants And Spices Extract" Research Foundation and Centre for Excellence in Nano Science and Technology , Synergy Institute of Technology," *Int. J. Plant, Anim. Environ. Sci.*, vol. 3, no. 1, pp. 68-78, 2012.

- [15] A. C. Larson and R. B. Von Dreele, "General Structure Analysis System," Los Alamos National Laboratory Report LAUR, 86-748, 2004.
- [16] B. H. Toby, "EXPGUI, A Graphical User Interface for GSAS," *J. Appl. Crystallogr.*, vol. 34, no. 2, pp. 210–213, 2001.
- [17] K. C. Maheswari and P. S. Reddy, "Green Synthesis of Magnetite Nanoparticles through Leaf Extract of *Azadirachta indica*," vol. 2, no. 4, pp. 189–191, 2016.
- [18] A. M. Awwad and N. M. Salem, "A Green and Facile Approach for Synthesis of Magnetite Nanoparticles," *Nanosci. Nanotechnol.*, vol. 2, no. 6, pp. 208–213, 2013.
- [19] V. S. Zaitsev, D. S. Filimonov, I. A. Presnyakov, R. J. Gambino, and B. Chu, "Physical and Chemical Properties of Magnetite and Magnetite-Polymer Nanoparticles and Their Colloidal Dispersions," *J. Coll. Inter. Sci.*, vol. 212, pp. 49–57, 1999.
- [20] H. M. Lu, W. T. Zheng, and Q. Jiang, "Saturation Magnetization of Ferromagnetic and Ferrimagnetic Nanocrystals at Room Temperature," *J. Phys. D. Appl. Phys.*, vol. 40, no. 2, pp. 320–325, 2007.